Role of Solvent and Secondary Doping in Polyaniline Films Doped with Chiral Camphorsulfonic Acid: Preparation of a Chiral Metal

Dean M. Tigelaar,[†] Wonpil Lee,[‡,1] Kenn A. Bates,[‡] Alexey Saprigin,[‡] Vladimir N. Prigodin,[‡] Xiaolin Cao,[§] Laurence A. Nafie,[§] Matthew S. Platz,*[,†] and Arthur J. Epstein*[,†,‡]

Department of Chemistry, The Ohio State University, Columbus, Ohio 43210-1185, Department of Physics, The Ohio State University, Columbus, Ohio 43210-1106, and Department of Chemistry, Syracuse University, Syracuse, New York 13244

Received November 12, 2001

We present the first study of chirality from the UV to the IR region for a conducting polymer, thereby probing the motion of the metallic "free carriers." Through study of chiral and achiral camphorsulfonic acid (CSA) doped polyaniline (PAN) films cast from different solvents (*m*-cresol and chloroform) and correlations with secondary doping experiments, we demonstrate that the chirality lies in the order "metallic" regions of the polymer films. Samples were studied by absorption, UV−vis−IR circular dichroism, and charge transport (temperature-dependent dc and microwave frequency conductivity and dielectric constant) measurements. The metallic films (cast from *m*-cresol) show strong optical activity of the conducting electrons in the visible and IR regions, showing that a chiral metal can be prepared by the methods of organic chemistry. In contrast, the nonmetallic chloroform cast films show weaker optical activity of the polymer backbone and a completely different interaction with CSA compared to *m*-cresol cast films. However, little difference in temperature-dependent dc conductivity is observed with PAN doped with chiral vs achiral CSA. It is postulated that chiral regions of the polymer backbone segregate in the metallic regions of the polymer film upon evaporation of *m*-cresol. Secondary doping of chloroform cast films with the vapors of *m*-cresol yields an increase in electron delocalization but a decrease in optical activity of the polymer backbone, in accord with a picture of inhomogeneous order in these materials.

Introduction

The area of conducting polymers has become a field of rapid growth[2] since the report of high conductivity in doped polyacetylene in 1977.[3] Extensive studies have been performed on materials such as polythiophenes,[4] polypyrroles,[5] poly(*p*-phenylene)s,[6] poly(*p*-pyridyl vinylene)s,[7] poly(*p*-phenylene vinylene)s,[8] and polyanilines.[9] Due to low cost and ease of processing, the use of these materials has been explored in many applications including light emitting devices,[10] lightweight batteries,[11] transistors,[12] photodiodes,[13] and sensors.[14]

Polyaniline (PAN) has received considerable interest because of its ease of synthesis, solubility, and the high

* To whom correspondence should be addressed.
[†] Department of Chemistry, The Ohio State University.
[‡] Department of Physics, The Ohio State University.
[§] Syracuse University.

(1) Present address: Samsung SDI 575 Shin-dong, PalDal-Gu, SuWon, Kyong-Gi, Korea 442-391.

(2) (a) *Handbook of Conducting Polymers*; Skotheim, T. A., Elsenbaumer, R. L., Reynolds, J. R., Eds.; Marcel Dekker: New York, 1998. (b) Blatchford, J. W.; Epstein, A. J. *Am. J. Phys.* **1996**, *64*, 120. (c) Epstein, A. J. *Springer Series in Materials Science*; Farchnni, R., Grosso, G. Eds.; **2001**, *41*, 3.

(3) (a) Chiang, C. K.; Fincher, C. R., Jr.; Park, Y. W.; Heeger, A. J.; Shirakawa, H.; Louis, E. J.; Gau, S. C.; MacDiarmid, A. G. *Phys. Rev. Lett.* **1977**, *39*, 1098. (b) Chiang, C. K.; Druy, M. A.; Gau, S. C.; Heeger, A. J.; Louis, E. J.; MacDiarmid, A. G.; Park, Y. W.; Shirakawa, H. *J. Am. Chem. Soc.* **1978**, *100*, 1013.

(4) (a) McCullough, R. D. *Adv. Mater.* **1998**, *10*, 93. (b) Roncali, J. *J. Mater. Chem.* **1999**, *9*, 1875. (c) McCullough, R. D.; Ewbank, P. C. In *Handbook of Conducting Polymers*; Skotheim, T. A., Elsenbaumer, R. L., Reynolds, J. R., Eds.; Marcel Dekker: New York, 1998; pp 225−258.

(5) (a) Reynolds, J. R.; Pyo, M.; Warren, L. F.; Marcy, H. O. *Synth. Met.* **1994**, *68*, 71. (b) Sotzing, G. A.; Reynolds, J. R.; Katritzky, A. R.; Soloducho, J.; Belyakov, S.; Musgrave, R. *Macromolecules* **1996**, *29*, 1679. (c) MacDiarmid, A. G. *Synth. Met.* **1997**, *84*, 27. (d) Zhou, M.; Heinze, J.; *J. Phys. Chem. B* **1999**, *103*, 8443. (e) Kohlman, R. S.; Joo, J.; Wang, Y. Z.; Pouget, J. P.; Kaneko, H.; Ishiguro, T.; Epstein, A. J. *Phys. Rev. Lett.* **1995**, *74*, 773.

(6) Berresheim, A. J.; Muller, M.; Mullen, K. *Chem. Rev.* **1999**, *99*, 1747.

(7) (a) Marsella, M. J.; Fu, D.; Swager, T. M. *Adv. Mater.* **1995**, *7*, 145. (b) Tain, J.; Wu, C.; Thompson, M. E.; Sturm, J. C.; Register, R. A. *Chem. Mater.* **1995**, *7*, 2190. (c) Blatchford, J. W.; Jessen, S. W.; Lin, L. B.; Lih, J. J.; Gustafson, T. L.; Epstein, A. J.; Fu, D. K.; Marsella M. J.; Swager, T. M.; MacDiarmid, A. G.; Yamaguchi, S.; Hamaguchi, M. J. *Phys. Rev. Lett.* **1996**, *76*, 1513. (d) Blatchford, J. W.; Jessen, S. W.; Lin, L. B.; Gustafson, T. L.; Fu, D. K.; Wang, H. L.; Swager, T. M.; MacDiarmid, A. G.; Epstein, A. J. *Phys. Rev. B* **1996**, *54*, 9180. (e) Li, X.; Cacialli, F.; Cervini, R.; Holmes, A. B.; Moratti, S. C.; Grimsdale, A. C.; Friend, R. H. *Synth. Met.* **1997**, *84*, 159.

(8) (a) Pakbaz, K.; Lee, C. H.; Heeger, A. J.; Hagler, T. W.; McBranch, D. *Synth. Met.* **1994**, *64*, 295. (b) Friend, R. H.; Denton, G. J.; Halls, J. J. M.; Harrison, N. T.; Holmes, A. B.; Koehler, A.; Lux, A.; Moratti, S. C.; Pichler, K.; Tessler, N.; Towns, K. *Synth. Met.* **1997**, *84*, 463.

(9) (a) MacDiarmid, A. G.; Epstein, A. J. *Faraday Discuss. Chem. Soc.* **1989**, *88*, 317. (b) Epstein, A. J.; MacDiarmid, A. G. *Synth. Met.* **1995**, *69*, 179. (c) Epstein, A. J.; MacDiarmid, A. G. *Mol. Cryst. Liq. Cryst.* **1988**, *160*, 165.

10.1021/cm011567x CCC: $22.00
Published on Web 02/28/2002

Scheme 1

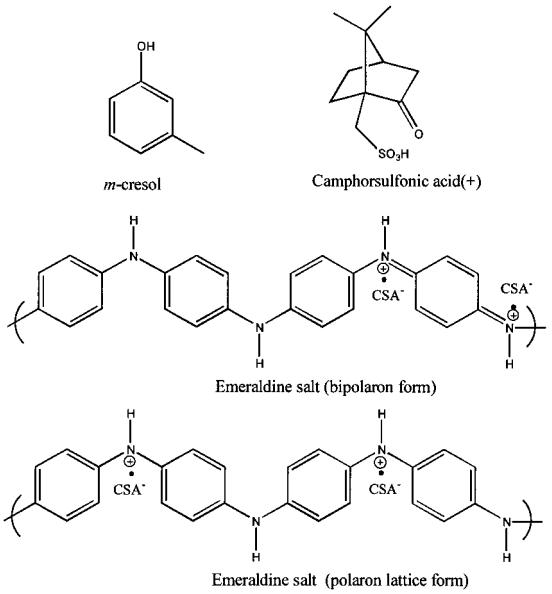

chemical and thermal stability of both its doped (conducting) and undoped (insulating) forms. The emeraldine salt form is the conducting form of polyaniline, which originates from protonation of the imine nitrogens of emeraldine base (EB), as shown in Scheme 1 in bipolaron and polaron lattice forms.[9,15] Films of emeraldine salt, prepared from emeraldine base films by doping with a strong acid, such as HCl, usually have a conductivity of 10^{-2} to 10^{1} S/cm at room temperature and become insulators at low temperature due to charge localization.[16] The conducting form of PAN becomes soluble in organic solvents when EB is protonated with a functionalized organic acid, such as camphorsulfonic acid (CSA).[17] It was shown that the choice of organic solvent is critical, with "good" solvents acting as "secondary dopants", which increase conductivity through increases in local structural order.[2c,15,18,19] In particular, *m*-cresol was shown to act as a good secondary dopant leading to conductivities up to 1000 times larger than that for PAN/CSA films prepared from chloroform.[17,18] Films of PAN/CSA cast from $CHCl_3$ are more disordered than those cast from *m*-cresol, have hopping conductivity, and become insulators at low temperature. PAN/CSA systems cast from *m*-cresol show metallic properties, such as a positive temperature coefficient of resistivity, a linear dependence of the thermoelectric power on temperature, and a metallic plasma frequency, with some samples remaining metallic to temperatures as low as 10 mK.[20] Computational studies by Ikkala et al. suggest that the phenolic group on *m*-cresol acts as a hydrogen-bonding donor to the carbonyl group on CSA while aligning itself above the PAN repeat units by van der Waals interactions.[21] This interaction acts to straighten the polymer chain, increasing the conjugation length and promoting crystallinity. Other solvents, like $CHCl_3$, do not allow for hydrogen-bonding interactions.

Another interesting aspect of CSA as a dopant is its optical activity. Minto and Vaughan have reported that films of PAN doped with a single enantiomer of CSA in *m*-cresol are more highly conductive and show increased metallic behavior.[22] They attribute this behavior to more favorable steric interactions of molecules in solution, leading to better packing on deposition. Furthermore, they report that PAN/CSA films cast from *m*-cresol are forced into a more planar, extended conformation in contrast with films cast from $CHCl_3$.[23]

On the basis of limited circular dichroism studies of PAN films doped with chiral CSA and cast from *m*-cresol, it was proposed that PAN is forced into a helical formation.[24] The circular dichroism of PAN/CSA dissolved in $CHCl_3$, DMF, DMSO, and NMP and from films cast from these solutions were reported by Wallace and co-workers.[25−27] Films cast from $CHCl_3$, DMF, DMSO, and NMP were all reported to have a similar chirality. These observed CD spectra are also attributed to helical formation of the polymer in solution. The data reflect the more localized electronic structure in solution.

(10) (a) Burroughes, J. H.; Bradley, D. C. C.; Brown, A. R.; Marks, R. N.; Mackay, K.; Friend, R. H.; Burns, P. L.; Holmes, A. B. *Nature* **1990**, *347*, 539. (b) Braun, D.; Heeger, A. J. *Appl. Phys. Lett.* **1991**, *58*, 1982. (c) Kraft, A.; Grimsdale, A. C.; Holmes, A. B. *Angew. Chem., Int. Ed.* **1998**, *37*, 402. (d) Friend, R. H.; Greenham, N. C. In *Handbook of Conducting Polymers*; Skotheim, T. A., Elsenbaumer, R. L., Reynolds, J. R., Eds.; Marcel Dekker: New York, 1998; pp 823−846. (e) Wang, Y. Z.; Epstein, A. J. *Acc. Chem. Res.* **1999**, *32*, 217.

(11) (a) Genies, E. M.; Hany, P.; Santier, C. J. *J. Appl. Electrochem.* **1988**, *18*, 285. (b) Kaneko, M.; Nakamura, H. *J. Chem. Soc., Chem. Commun.* **1985**, 346.

(12) (a) Lovinger, A. J.; Rothberg, L. J. *J. Mater. Res.* **1996**, *11*, 1581. (b) Garnier, F. *Chem. Phys.* **1998**, *227*, 253. (c) Schon, J. H.; Dodabalapur, A.; Bao, Z.; Kloc, C.; Schenker, O.; Batlogg, B. *Nature* **2001**, *410*, 189.

(13) (a) Sariciftci, N. S.; Smilowitz, L.; Heeger, A. J.; Wudl, F. *Science* **1992**, *258*, 1474. (b) Yu, G.; Heeger, A. J. *J. Appl. Phys.* **1995**, *78*, 4510. (c) Yu, G.; Gao, J.; Hummelen, J. C.; Wudl, F.; Heeger, A. J. *Science* **1995**, *270*, 1789.

(14) Guiseppi-Elie, A.; Wallace, G. G. In *Handbook of Conducting Polymers*; Skotheim, T. A., Elsenbaumer, R. L., Reynolds, J. R., Eds.; Marcel Dekker: New York, pp 963−992.

(15) (a) Jozefowicz, M. E.; Laversanne, R.; Javadi, H. H. S.; Epstein, A. J.; Pouget, J. P.; Tang, X.; MacDiarmid, A. G.; *Phys. Rev. B.* **1989**, *39*, 12958. (b) Pouget, J. P.; Jozefowicz, M. E.; Epstein, A. J.; Tang, X.; MacDiarmid, A. G. *Macromolecules* **1991**, *24*, 779.

(16) (a) Wang, Z. H.; Li, C.; Scherr, E. M.; MacDiarmid, A. G.; Epstein, A. J. *Phys. Rev. Lett.* **1991**, *66*, 1745. (b) Wang, Z. H.; Scherr, E. M.; MacDiarmid, A. G.; Epstein, A. J. *Phys. Rev. B* **1992**, *45*, 4190. (c) Joo, J.; Oblakowski, Z.; Du, G.; Pouget, J. P.; Oh, E. J.; Wiesinger, J. M.; Min, Y.; MacDiarmid, A. G.; Epstein, A. J. *Phys. Rev. B.* **1994**, *49*, 2977. (d) Joo, J.; Du, G.; Prigodin, V. N.; Tsukamoto, J.; Epstein, A. J. *Phys. Rev. B* **1995**, *52*, 8060.

(17) Cao, Y.; Smith, P.; Heeger, A. J. *Synth. Met.* **1992**, *48*, 91.

(18) (a) MacDiarmid, A. G.; Epstein, A. J. *Synth. Met.* **1994**, *65*, 103. (b) Younan, X.; MacDiarmid, A. G.; Epstein, A. J. *Macromolecules* **1994**, *27*, 7212. (c) Xia, Y.; Wiesinger, J. M.; MacDiarmid, A. G.; Epstein, A. J. *Chem. Mater.* **1995**, *7*, 443. (d) MacDiarmid, A. G.; Epstein, A. J. *Synth. Met.* **1995**, *69*, 85. (e) Min, Y.; Xia, Y.; MacDiarmid, A. G.; Epstein, A. J. *Synth. Met.* **1995**, *69*, 159.

(19) Pouget, J. P.; Obakowski, Z.; Nogami, Y.; Albouy, P. A.; Laridjani, M.; Oh, E. J.; Min, Y.; MacDiarmid, A. G.; Tsukamoto, J.; Ishiguro, T.; Epstein, A. J. *Synth. Met.* **1994**, *65*, 131.

(20) Kohlman, R. S.; Zibold, A.; Tanner, D. B.; Ihas, G. G.; Ishiguro, T.; Min, Y. G.; MacDiarmid, A. G.; Epstein, A. J. *Phys. Rev. Lett.* **1997**, *78*, 3915.

(21) (a) Ikkala, O. T.; Pietila, L.; Ahjopalo, L.; Osterholm, H.; Passiniemi, P. J. *J. Chem. Phys.* **1995**, *103*, 9855. (b) Vikki, T.; Pietila, L.; Osterholm, H.; Ahjopalo, L.; Takala, A.; Toivo, A.; Levon, K.; Passiniemi, P. J.; Ikkala, O. T. *Macromolecules* **1996**, *29*, 2945.

(22) Minto, C. D. G.; Vaughan, A. S. *Polymer* **1997**, *38*, 2683.

(23) Minto, C. D. G.; Vaughan, A. S. *Synth. Met.* **1998**, *93*, 73.

(24) Havinga, E. E.; Bouman, M. M.; Meijer, E. W.; Pomp, A.; Simenon, M. M. J. *Synth. Met.* **1994**, *66*, 93.

(25) (a) Majidi, M. R.; Kane-Maguire, L. A. P.; Wallace, G. G. *Polymer* **1994**, *35*, 3113. (b) Majidi, M. R.; Kane-Maguire, L. A. P.; Wallace, G. G. *Polymer* **1995**, *36*, 3597. (c) Majidi, M. R.; Kane-Maguire, L. A. P.; Wallace, G. G. *Polymer* **1996**, *37*, 359.

(26) (a) Majidi, M. R.; Ashraf, S. A.; Kane-Maguire, L. A. P.; Norris, I. D.; Wallace, G. G. *Synth. Met.* **1997**, *84*, 115. (b) Norris, I. D.; Kane-Maguire, L. A. P.; Wallace, G. G. *Macromolecules* **1998**, *31*, 6529.

(27) (a) Innis, P. C.; Norris, I. D.; Kane-Maguire, L. A. P.; Wallace, G. G. *Macromolecules* **1998**, *31*, 6521. (b) Norris, I. D.; Kane-Maguire, L. A. P.; Wallace, G. G. *Macromolecules* **2000**, *33*, 3237.

Surprisingly, there has not been a thorough study comparing films doped with optically active CSA and cast from $CHCl_3$ vs *m*-cresol, even though these films have such varying properties. The present study was undertaken to better understand the ramifications for films doped with chiral CSA and cast from *m*-cresol and $CHCl_3$. Thus, absorption and CD measurements were extended into the IR region to better observe the delocalized electrons in highly conductive PAN. These delocalized electrons are primarily associated with the formation of ordered regions in the doped polymer.[18,19,20] These studies are complemented by dc and microwave frequency charge transport measurements in films doped with both chiral and racemic CSA. Furthermore, the first study of the effects of secondary doping on polymer chirality was undertaken. PAN/CSA films cast from $CHCl_3$ were studied both before and after secondary doping with *m*-cresol vapors by absorption, CD, and transport measurements. We conclude that the nonmetallic PAN/CSA films cast from $CHCl_3$ have little chirality. When the films are exposed to secondary doping with *m*-cresol vapors, the PAN chains begin to straighten out and lose their limited optical activity. We also conclude that for films that are cast from *m*-cresol, optical activity originates in the metallic (more ordered) regions of the films. An intermolecular interaction between polymer chains is proposed.

Experimental Section

m-Cresol was purchased from Aldrich and used as received. Chloroform was purchased from Fisher and also used as received. PAN was synthesized at −25 °C according to Monkman's procedure.[28] Molecular weight values that they obtained in their synthesis were 153 000, 209 000, 43 500, and 4.8 for M_p, M_w, M_n, and polydispersity, respectively. In a typical experiment for making films, a 2:1 ratio of CSA to EB repeat unit was ground together with a mortar and pestle and then dissolved in the appropriate solvent to make a solution that was 2.7 wt % EB + CSA. The solution was then mixed with an IKA Labortechnik T25 basic homogenizer at 20 000 rpm for 10 min and centrifuged for 30 min. Solutions were generally allowed to gelate for 1−2 h before making films. Changes in gelation time[29] made little to no difference in the appearance of absorption or CD spectra. Thin films were made by spin-casting the solution on either a quartz or BaF_2 substrate at 500 rpm for 30 s and then from 1000 to 3000 rpm for 60 s, depending upon the solution viscosity and desired film thickness. Thick films (∼40 μm) for transport measurements were drop-cast on silicon wafers at the same time spin-cast films were made, dried in an oven at 80 °C for 1−2 days, and peeled off. Visible CD spectra were taken using a Jasco J-500C spectropolarimeter. For our method of preparation, films cast from less than 2 wt % solutions from *m*-cresol showed no CD spectrum. Electronic UV−vis−near-IR absorption spectra were taken with the same samples using a Perkin-Elmer λ-19 spectrometer. IR absorption and vibrational circular vibrational (VCD) spectra were taken using a mid-IR Fourier transform VCD spectrometer, the Chiralir from Bomem/BioTools.[30] The instrument includes an external VCD bench, constructed in-house and equipped with two ZnSe photoelastic modulators from Hinds Instruments that were used for all spectral measurements. The dual polarization modulation technique[31] was employed on the VCD bench to suppress artifacts introduced by small amounts of stray linear birefringence in the optical components of the instrument. The spin-coated film samples were checked for birefringence and were found to have none of significance within the sensitivity range of these measurements. This is also indicated by the mirror-image symmetry, relative to zero VCD, of chiral films induced by mirror-image chiral molecules and by the flat VCD baseline obtained for films cast with racemic mixtures of chirality-inducing molecules. The sensitivity of the instrument was optimized for the frequency regions of interest, and all IR and VCD spectra were recorded at the resolution of 4 cm^{-1}. Temperature-dependent dc conductivity and microwave measurements at 6.5 GHz were performed utilizing the four-probe[32] and cavity perturbation[33] methods, respectively. Secondary doping was done by filling the bottom of a closed vessel with *m*-cresol and suspending the chloroform cast films 1 in. above the solution. The amount of exposure time was varied from 1 h to 3 days. However, the amount of exposure time had little effect on the appearance of CD spectra.

Results and Discussion

MacDiarmid, Epstein, and co-workers proposed that doped PAN, in films cast from $CHCl_3$, is "compact coil" in nature, resulting in localized polarons being confined to short conjugation lengths.[18] In films cast from *m*-cresol, PAN exists in an expanded coil form. The localized polaron absorption is replaced by a "free carrier tail" absorption due to the delocalized electrons. This proposal accounts for the UV−vis−near-IR absorption spectra from PAN/CSA(+) shown in Figure 1. Chloroform cast films show three distinct peaks at 360, 440, and 800 nm, which correspond to transitions from the π to π^* band, localized polaron to π^* band, and the π to polaron band, respectively.[34] For the *m*-cresol cast films, the localized polaron band at 800 nm is replaced by broad intraband transitions within the half-filled delocalized polaron band (free carrier tail), which extends from 520 nm to beyond 2500 nm. This free carrier tail extends further into the IR, as can be seen from the IR absorption spectra shown in Figure 2.[20]

MacDiarmid, Epstein, and co-workers also reported that when chloroform cast PAN/CSA films are exposed to the vapors of *m*-cresol, the localized polaron spectrum is gradually replaced by the *m*-cresol-like expanded coil spectrum.[18] This phenomenon is known as secondary doping. To further understand the morphology of PAN/CSA films, chloroform cast films from CSA(+) were exposed to secondary doping. The final absorption spectrum in Figure 1 shows the $CHCl_3$ cast film after being exposed to *m*-cresol vapors for 3 days.

The absorption spectra, accompanied by circular dichroism spectra taken in the UV−vis and IR regions,

(28) Adams, P. N.; Laughlin, P. J.; Monkman, A. P.; Kenwright, A. M.; *Polymer* **1996**, *37*, 3411.

(29) Oh, E. J.; Min, Y.; Wiesinger, J. M.; Manohar, S. K.; Scherr, E. M.; Prest, P. J.; MacDiarmid, A. G.; Epstein, A. J. *Synth. Met.* **1993**, *55*, 977.

(30) (a) Nafie, L. A. *Annu. Rev. Phys. Chem.* **1997**, *48*, 357. (b) Nafie, L. A.; Freedman, T. B *Enantiomer* **1998**, *3*, 283. (c) Nafie, L. A.; Freedman, T. B. In *Circular Dichroism, Theory and Practice*; Nakanishi, K., Berova, N., Woody, W., Eds.; Wiley: New York, 2000; pp 97−131. (d) Nafie, L. A. In *Encyclopedia of Spectroscopy*; Linden, J. C., Tranter, G. E., Holmes, J. L., Eds.; Academic Press: London, 2000; pp 2391−2402. (e)) Nafie, L. A.; Freedman, T. B. In *Infrared and Raman Spectroscopy of Biological Materials*; Yan, B., Gremlish, H.-U., Eds.; Marcel Dekker: New York, 2001; pp 15−54. (f) Dukor, R. K.; Nafie, L. A. In *Encylopedia of Analytical Chemistry: Instrumentation and Applications*; Meyers, R. A., Ed.; John Wiley and Sons: Chichester, 2000; pp 662−676.

(31) Nafie, L. A. *Appl. Spectrosc.* **2000**, *54*, 1634−1645.

(32) Zuo, F.; Angelopoulos, M.; MacDiarmid, A. G.; Epstein, A. J. *Phys. Rev. B* **1987**, *36*, 3475.

(33) Javadi, H. H. S.; Cromack, K. R.; MacDiarmid, A. G.; Epstein, A. J. *Phys. Rev. B* **1989**, *39*, 3579.

(34) Stafstrom, S.; Bredas, J. L.; Epstein, A. J.; Woo, H. S.; Tanner, D. B.; Huang, W. S.; MacDiarmid, A. G. *Phys. Rev. Lett.* **1987**, *59*, 1464.

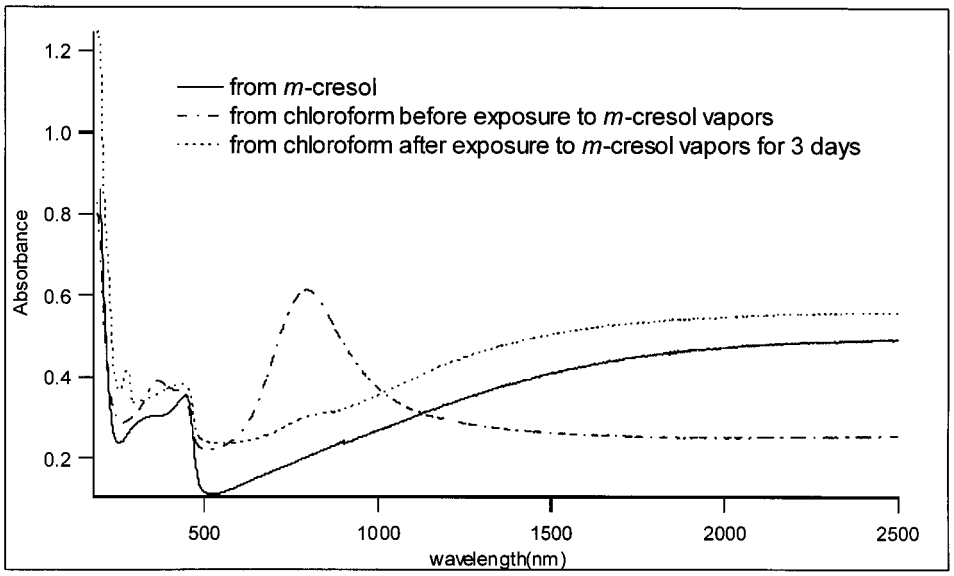

Figure 1. Absorption spectra of 2.7 wt % PAN/CSA(+) spin-cast from *m*-cresol and spin cart from $CHCl_3$ before and after exposure to *m*-cresol vapors for 3 days.

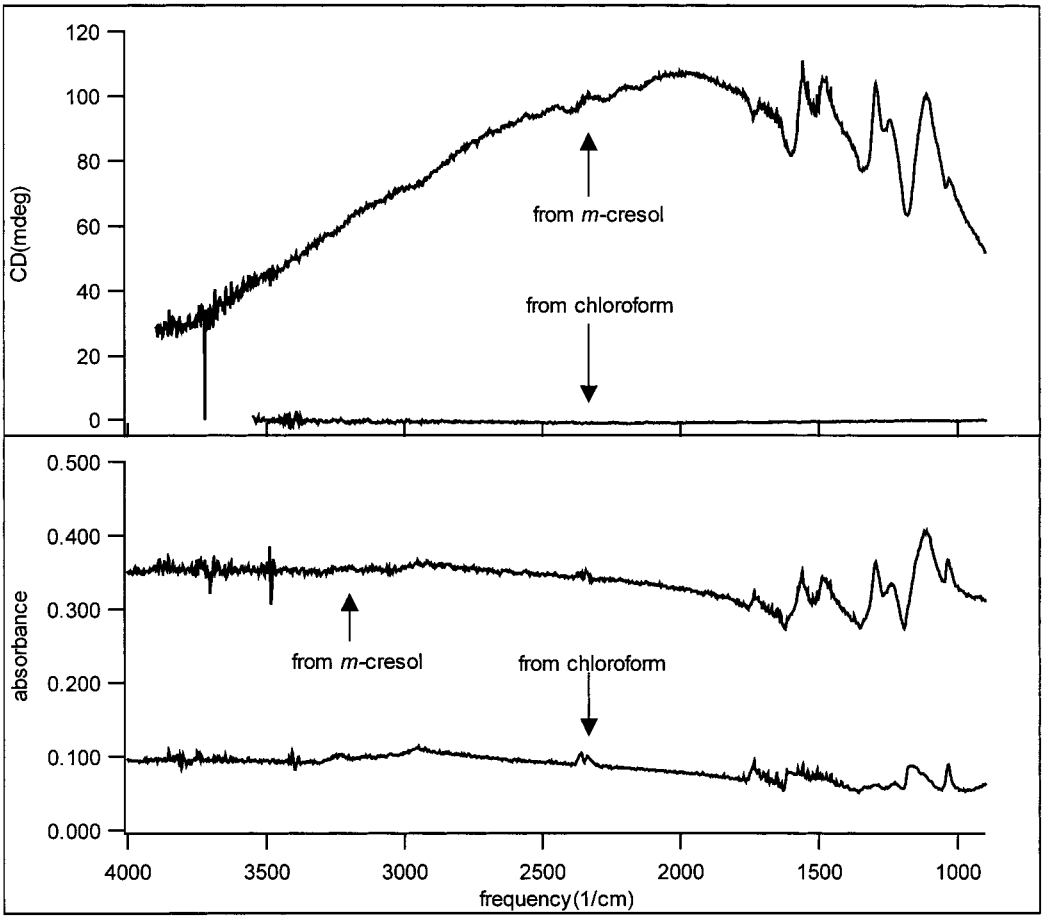

Figure 2. IR absorption and circular dichroism in reciprocal centimeters of PAN/CSA(+) cast from *m*-cresol and chloroform.

are shown in Figures 2, 3, and 4.[35] Figure 3 shows the CD spectra of *m*-cresol cast films of PAN/CSA(+), PAN/CSA(−), and PAN/CSA(±) from 190 to 12 500 nm. Instrumentation was not available to cover the 1000−2270 nm spectral range. The visible CD spectrum is expanded as an insert in Figure 3. Figure 4 shows the CD spectra of $CHCl_3$ cast films in both the visible and the IR regions. The visible CD spectrum is expanded as an insert in Figure 4.

Comparison of these two CD spectra lead to several observations: (1) Doping with CSA(+) vs CSA(−) leads to an induced optical activity of equal but opposite sign throughout the measured spectrum, independent of the

(35) (a) *Optical Rotatory Dispersion*; Djevassi, C., Ed.; McGraw-Hill: New York, 1960. (b) *Optical Circular Dichroism*; Velluz, L., Legrand, M., Grosjean, M., Eds.; Academic Press: New York, 1965.

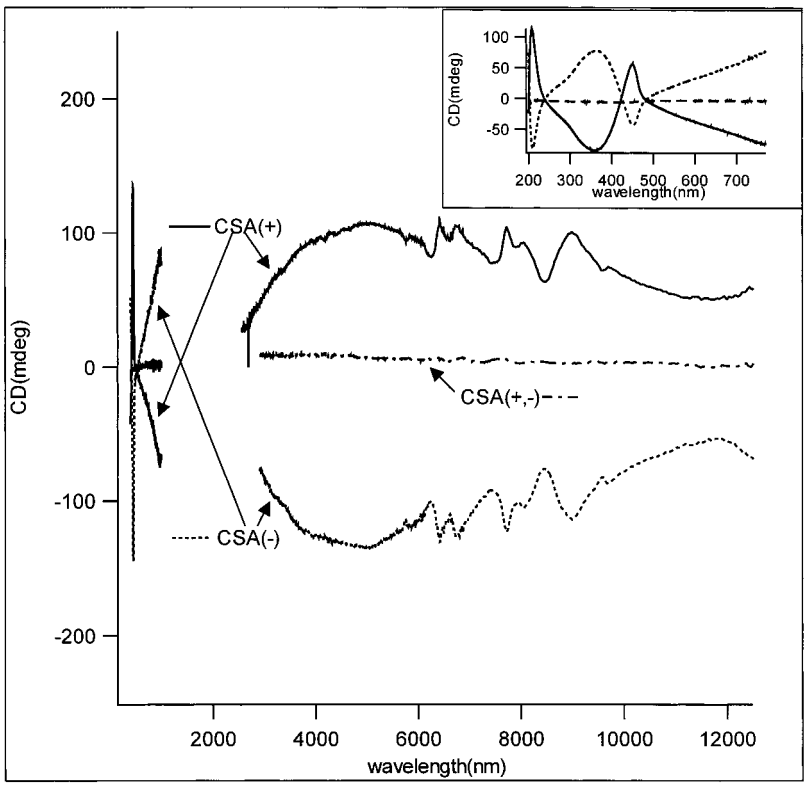

Figure 3. Visible and IR circular dichroism spectra of PAN/CSA(+), PAN/CSA(−), and PAN/CSA(+,−) cast from *m*-cresol. Insert: closeup of CD spectra in the visible region.

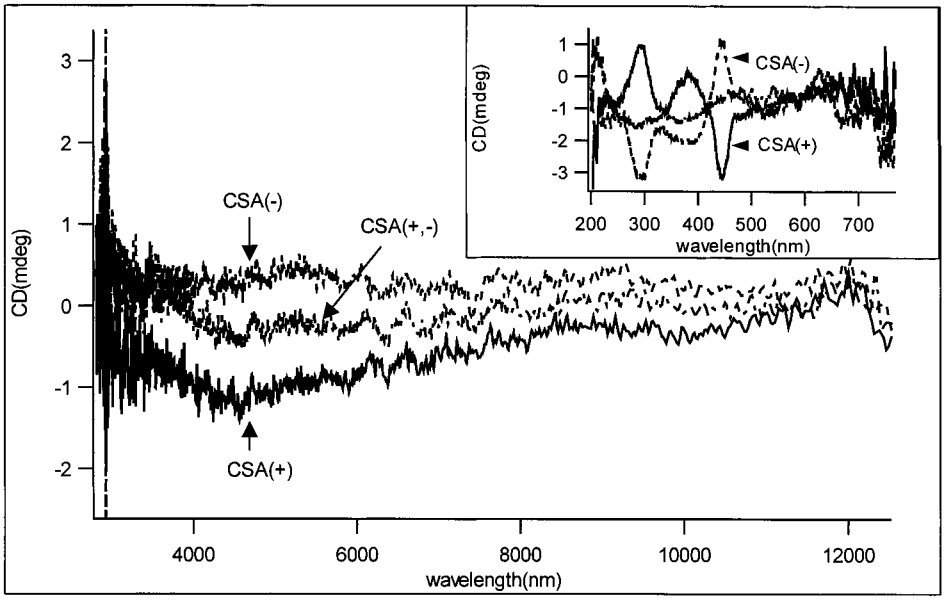

Figure 4. Visible and IR circular dichroism spectra of PAN/CSA(+), PAN/CSA(−), and PAN/CSA(+,−) cast from chloroform. Insert: closeup of CD spectra in the visible region.

solvent used in film preparation. The weak Cotton effects[35] associated with CSA itself can be seen at 290 nm for the $CHCl_3$ cast films and the carbonyl stretch at 5780 nm (1730 cm^{-1}) in *m*-cresol cast films. All other optical activity observed in these spectra results from the induced optical activity of the PAN chains. (2) Although all films are of comparable thickness, Cotton effects observed from *m*-cresol cast films are 100 fold larger than those from $CHCl_3$ cast films. The increased Cotton effect is associated with the dramatically larger structural order induced in the PAN/CSA backbone due to interactions in the presence of *m*-cresol than for $CHCl_3$ cast films. (3) Cotton effects at 360 and 440 nm for the films are of opposite sign for the same enantiomer of CSA for the two different casting solvents. Thus, the PAN/CSA interaction that induces chirality in the polymer backbone must be completely different in the two solvents. This contrasts with the earlier report of Wallace and co-workers that spectra of films cast from DMF, NMP, and DMSO are similar to $CHCl_3$ in appearance.[25,26,27] One may propose that since $CHCl_3$ is more volatile than *m*-cresol, differences in CD spectra

Table 1. Observed Transitions in PAN/CSA(+)

peak/nm (cm^{-1})	solvent	Cotton effect	origin	reference
350	$CHCl_3$	+	π to π^* band	34
350	*m*-cresol	−	π to π^* band	34
440	$CHCl_3$	−	polaron to π^* band	34
440	*m*-cresol	+	polaron to π^* band	34
~800	$CHCl_3$	none	π band to polaron band	34
500−near ir	*m*-cresol	split	π band to conduction band and intra-conduction band	34
6250(1600)	$CHCl_3$	none	quinoid ring stretch	38
6410(1560)	*m*-cresol	+	protonated quinoid ring stretch	38
6760(1480)	*m*-cresol	+	protonated quinoid ring stretch	38
7720(1295)	*m*-cresol	+	C−N stretch + C−H bend of protonated quinoid ring	38
7750(1290)	$CHCl_3$	none	C−N stretch + C−H bend of EB unit	38
8030(1245)	*m*-cresol	+	C−N stretch + C−C stretch of protonated EB	38
8620(1160)	$CHCl_3$	none	C−H in-plane bend of EB unit	38
8970(1115)	*m*-cresol	+	C═N stretch of protonated quinoid ring	38

may be due to different amounts of residual solvent left in the polymer films. We can further look at the CD spectra in solution to demonstrate the different interactions of PAN with CSA in these two solvents. Optically active PAN/CSA exhibits a CD spectrum in solution in $CHCl_3$ but not in *m*-cresol. Majidi et al. even show that when *m*-cresol is added to $CHCl_3$ solution, optical activity disappears.[26a] We have further observed that even in PAN/CSA films that are cast from *m*-cresol, films had to be cast from a concentration of 2 wt % or higher to have any optical activity. (4) The Cotton effect measured in the free carrier tail shows "exciton-like" splitting[36] by changing sign between the visible and IR regions. Although it is not shown, extrapolation of the CD spectra in Figure 3 leads to a crossover in sign around 2000 nm. This observation leads to a pair of possible interpretations. The highly conductive regions of PAN/CSA films cast from *m*-cresol could deposit in right and left-handed helixes, as proposed for PAN/CSA in $CHCl_3$ solutions and in $CHCl_3$ cast films. Alternatively, Ikkala and co-workers proposed that interactions between PAN, CSA, and *m*-cresol lead to chiral, extended polymer chains that are coupled to each other and interact with light as separate chromophores.[21] A similar structure has been proposed previously to describe regioregular polythiophenes with chiral side chains.[37]

The IR spectrum of the *m*-cresol cast film is given in Figure 2 and shows 6 distinct vibrational absorptions between 1600 and 1000 cm^{-1}, in accord with earlier reports for vibrations in the emeraldine salt.[38,39][39] Each of these peaks are accompanied by a Cotton effect in the CD spectrum. Although much weaker, the chloroform cast films also show several peaks in the IR, which correspond to the emeraldine base form of PAN. However, none of these peaks lead to a Cotton effect. These results lead us to believe that in these films, optical activity is induced almost exclusively in the highly conducting (structurally ordered) regions of the polymer. For the sake of clarity, all of the observed peaks are reported in Table 1 in both nm and cm^{-1}, along with the sign of the Cotton effect and the origin of the signal. It is noted that the IR peaks of the *m*-cresol cast film have the "Fano" shape[40] expected for interaction between a discrete absorption (the vibrational mode) and a continuous absorption (from the free carrier tail of the delocalized polaron band), further supporting that the chiral activity is associated with ordered (metallic) regions of the chiral CSA doped PAN.

Charge transport and dielectric data for thicker films of the same composition are shown in Figures 6, 7, and 8. Room-temperature dc conductivities (σ(300 K)) of PAN/CSA(+,−) and PAN/CSA(+) films cast from *m*-cresol were ~150 and 170 S/cm with σ(10 K)/σ(300 K) ~ 0.56 and 0.62, respectively. Temperature dependences of PAN doped with a single enantiomer and a racemic mixture of CSA are very similar with the single enantiomer having a sharper maximum. These results are similar to those reported by Minto and Vaughan,[22] though their PAN/CSA(+) sample has a larger room-temperature conductivity. Our $\sigma_{dc}(T)$ results for both enantiomerically pure and racemically doped samples are similar. We attribute the subtle difference in results to the different ways in which the polymer films were made and processed between the two groups. A temperature-dependent reduced activation energy $W(T)$ (defined as d log $\sigma(T)$/d log T) plot from $\sigma_{dc}(T)$, inset Figure 6, shows a metallic behavior below 10 K for both racemic and enantiomerically pure samples. A crossover from negative to positive $W(T)$ slope upon cooling indicates that both films are "metallic" .[20]

Microwave conductivity $\sigma_{mw}(T)$ of PAN/CSA(+,−) and PAN/CSA(+) films cast from *m*-cresol shows a similar temperature dependence to the dc conductivity with room-temperature conductivity values of 300 and 410 S/cm, respectively. Figure 8 shows a very large negative microwave frequency dielectric constant with similar temperature dependences for PAN doped with a single enantiomer and a racemic mixture of CSA. No significant difference is observed between PAN/CSA(+,−) and PAN/CSA(+) from *m*-cresol, although PAN−CSA(+)/*m*-cresol shows a slightly weaker temperature dependence. This indicates that in microwave frequency range (6×10^9 Hz) chirality does not substantially affect the charge conduction process. The negative dielectric constant (ϵ_{mw}) of -7×10^4 and -5.5×10^4 for PAN−CSA(+,−) and PAN/CSA(+), respectively, at 300 K suggest a Drude-like dielectric response at microwave frequency.[16]

(36) *Circular Dichroic Spectroscopy*; Harada, N., Nakanishi, K., Eds.; Oxford University Press: Oxford, 1983.
(37) Bouman, M. M.; Meijer, E. W.; *Polymer Prepr.* **1994**, *35*, 309.
(38) (a) Tang, J.; Jing, X.; Wang, B.; Wang, F. *Synth. Met.* **1988**, *24*, 231. (b) Harada, I.; Furukawa, Y.; Ueda, F.; *Synth. Met.* **1989**, *29*, E303.
(39) (a) Asturias, G. E.; MacDiarmid, A. G.; McCall, R. P.; Epstein, A. J. *Synth. Met.* **1989**, *29*, E157. (b) Colomban, P.; Gruger, A.; Novak, A.; Regis, A. *J. Mol. Struct.* **1994**, *317*, 261.
(40) McCall, R. P.; Roe, M. G.; Ginder, J. M.; Kusumoto, T.; Epstein, A. J.; Asturias, G. E.; Scherr, E. M.; MacDiarmid, A. G. *Synth. Met.* **1989**, *29*, E433.

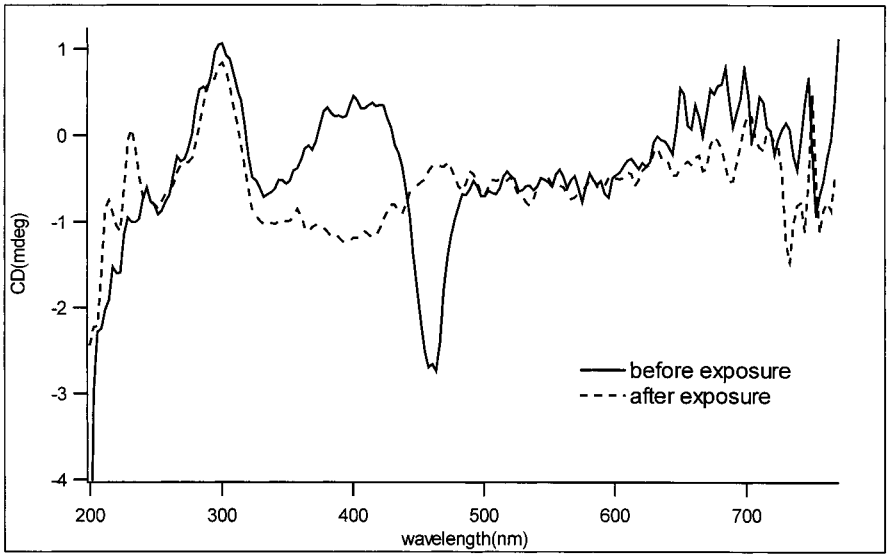

Figure 5. Visible circular dichroism spectrum of PAN/CSA(+) cast from chloroform before and after secondary doping with *m*-cresol vapors for 3 days.

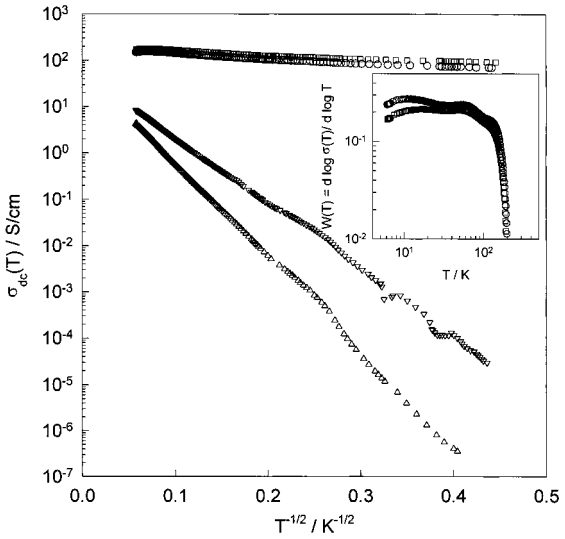

Figure 6. The dc conductivity of PAN−CSA(+,−)/*m*-cresol (○) and (+)/*m*-cresol (□) and (+)/$CHCl_3$ before (△) and after (▽) *m*-cresol treatment. Inset: log−log plot of $\omega(T)$ vs T for PAN−CSA(+,−) and PAN−CSA(+) cast from *m*-cresol.

The ϵ_{max} remains negative down to 10 K. These results are similar to those for hexafluorophosphate polypyrrole [PPy(PF_6)][5e,20] and highly conducting PAN/CSA.[20,41] The microwave frequency data can be fit using the Drude model at the low-frequency limit ($\omega\tau \ll 1$), $\sigma_{mw} \sim (\omega_p 2/4\pi)/\tau$ and $\epsilon_{mw} \sim -\omega_p 2\tau^2$. Hence, ω_p and τ ($\sim 4\pi\epsilon_{mw}/\sigma_{mw}$) are ∼0.008, 0.01 eV (∼30 cm^{-1}) and ∼2.0 × 10^{-11}, 1.6 × 10^{-11} s, for PAN/CSA(+,−) and PAN/CSA(+), respectively. This small ω_p likely originates from the most delocalized electrons of the conduction band.[20] Earlier studies of PAN showed that the polymer films consist of highly conductive ordered metallic regions ("islands") surrounded by a sea of disordered, less conductive material.[16,42] The conductivities of films are ultimately determined by the transit of charges between the metallic islands. The anomalously long τ in these samples reflects the time for metallic electrons to transit the disordered regions. If we assume that all of the chirality induced in PAN is within the metallic regions, this explains the similar $\sigma_{dc}(T)$ and $\sigma_{mw}(T)$ values, even though a single enantiomer of CSA creates chiral structural order in the polymer backbone. Furthermore, it is noted that the room-temperature conductivity of the *m*-cresol cast films are greater than that of the $CHCl_3$ cast films by about a factor of 100, identical to the difference in the magnitude of the CD spectra. The results, combined with exciton splitting of the free carrier tail and the Cotton effects observed in the IR spectra, lead us to believe that optical activity in *m*-cresol cast films is induced primarily within the ordered metallic islands.

More information can be obtained by a further look at the CD and transport data of PAN/CSA(+) and PAN/CSA(±) cast from $CHCl_3$ before and after exposure to *m*-cresol vapors. Although secondary doping induces a large free carrier tail in the absorption spectrum, this broad absorption shows no induced chirality, as shown in Figure 5. In fact, after exposure to *m*-cresol vapors from a few hours to 3 days, the Cotton effects at 360 and 440 nm almost disappear completely. These observations lead to the conclusion that once the film is prepared, the polymer chirality is "locked" into place. The addition of *m*-cresol may act to straighten out the polymer chain to some extent, but CSA cannot rearrange to create the same interaction present in films cast from *m*-cresol. In fact, the straightening out of the polymer chains by *m*-cresol appears to remove any chiral interaction that CSA had induced in the PAN. Xia et al. have shown previously that secondary doping induces a permanent alteration in the polymer chains. They report that the UV−vis−near-IR spectra and surface resistance of the films remain unchanged even after heating the films or dipping them in acetone for several minutes.[18b] Therefore, secondary doping is a way to permanently remove chirality from optically active PAN/CSA films cast from $CHCl_3$. If we assume the

(41) Kohlman, R. S.; Joo, J.; Min, Y. G.; MacDiarmid, A. G.; Epstein, A. J. *Phys. Rev. Lett.* **1996**, *77*, 2766.

(42) (a) Wang, Z. H.; Ray, A.; MacDiarmid, A. G.; Epstein, A. J. *Phys. Rev. B* **1991**, *43*, 4373. (b) Pouget, J. P.; Jozefowicz, M. E.; Epstein, A. J.; Tang, X.; MacDiarmid, A. G. *Macromolecules* **1991**, *24*, 779. (c) Prigodin, V. N.; Epstein, A. J. *Synth. Met.* **2002**, *125*, 43.

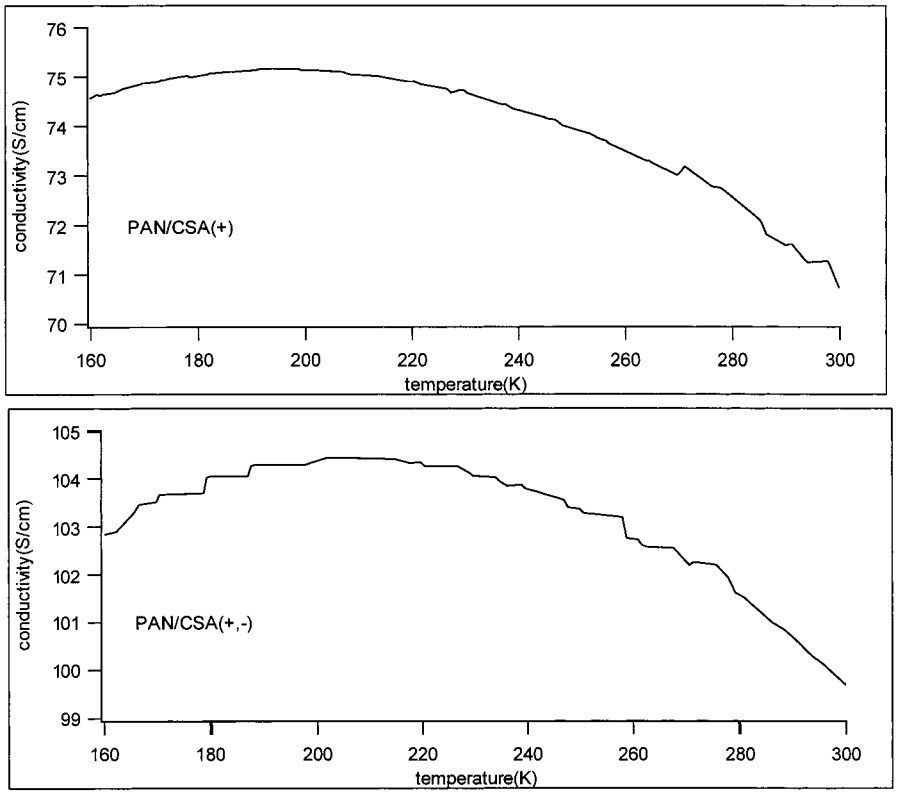

Figure 7. The dc conductivity of PAN−CSA(+) and PAN−CSA(+,−) vs temperature. (Note: "steps" are due to digitization of the data.)

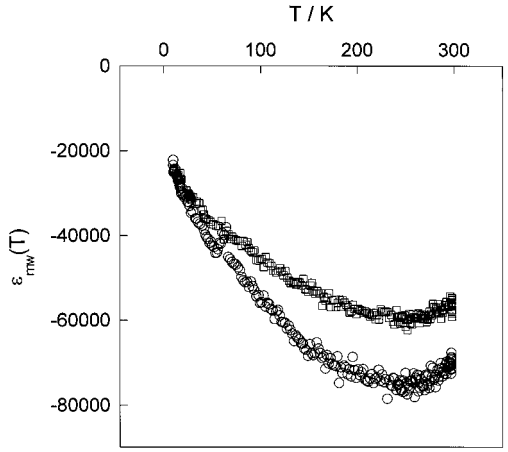

Figure 8. Microwave dielectric constant of PAN−CSA(+,−)/*m*-cresol (○) and (+)/*m*-cresol (□) films.

model of Wallace and co-workers that PAN/CSA forms a helical structure from $CHCl_3$,[25,26,27] our results suggest that *m*-cresol then acts to elongate the helix and thus move the backbone away from the interaction with CSA. From the transport data shown in Figure 6, $\sigma_{dc}(T)$ of $CHCl_3$ cast PAN/CSA(+) films both before and after *m*-cresol vapor treatment can be well fitted by quasi-1D VRH conduction mechanism ($\sigma(T) = \sigma_0 \exp[-(T_0/T)^{1/2}]$).[43] σ(300 K) ∼ 4.1 and 8.3 S/cm and T_0 ∼ 2100 and 1100 K before and after *m*-cresol treatment, respectively. These results also provide support to the secondary doping by *m*-cresol vapors straightening any helical arrangement in the polymer backbone.

A final experiment was run in which the IR CD spectra were compared for *m*-cresol cast films, in which one film contains 100% CSA(+) and the other film contains only a 5% excess of CSA(+) (52.5:47.5 CSA-(+)/CSA(−)). To account for differences in film thickness, a plot of CD/absorbance vs wavelength was made, as shown in Figure 9. This plot contains the spectra of the two films mentioned above and a final spectrum of the film with 5% excess CSA(+) multiplied by a factor of 20 to mimic the enantiomerically pure sample. The CD in the free carrier tail is much greater than expected, which is around 8000 nm or a conjugation length of approximately 5−6 repeat units.[44] This is a relatively short conjugation length but is longer than what would be predicted if CSA(+) and CSA(−) associated with PAN randomly. These results support the proposal that CSA enantiomers preferentially self-aggregate in the preparation of PAN films.

Conclusions

Absorption, circular dichroism, and transport measurements of PAN/CSA films cast from $CHCl_3$ support the proposal that under these processing conditions, PAN/CSA is strongly disordered with a modest chirality. This proposal is supported by charge transport measurements of films that match a Q1D-VRH mechanism, both before and after secondary doping. This type of structure would be expected to have short conjugation lengths, as shown by the UV−vis and IR spectra. When secondary doping is applied to these films by exposure

(43) Epstein, A. J.; Lee, W. P.; Prigodin, V. N. *Synth. Met.* **2001**, *117*, 9.

(44) 8000 nm = 3.8×10^{13} s^{-1}. Assuming that the Fermi velocity of the delocalized electron is 10^5 m/s, the distance traveled by the electron at 8000 nm ≈ 10^5 m/s × (1 s/3.8×10^{13}) ≈ 25−30 Å.

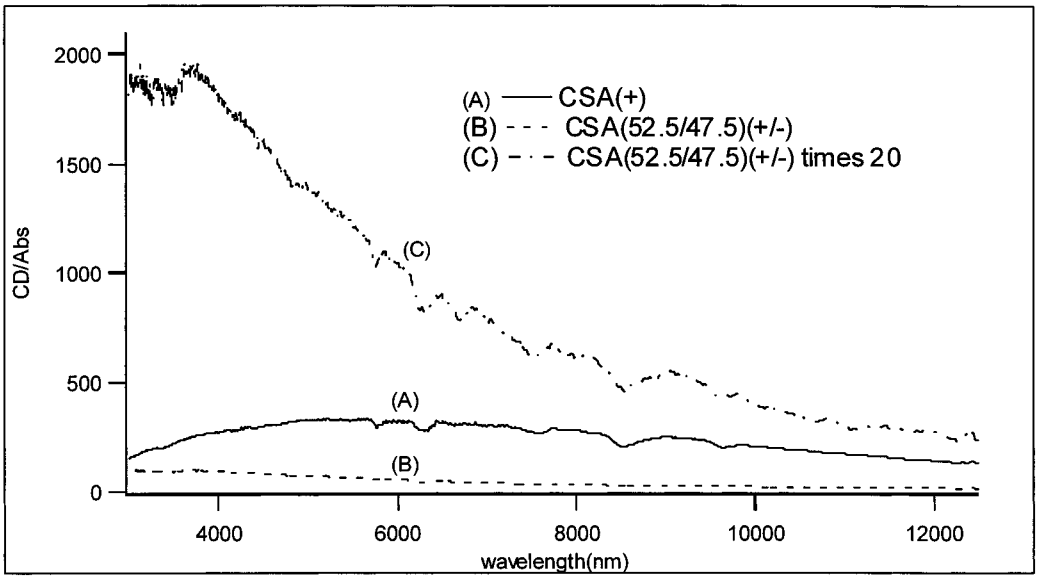

Figure 9. CD/absorbance spectrum of films of 2.7 wt % polyaniline cast from *m*-cresol doped with pure CSA(+) (A) and a 52.5:47.5 ratio of CSA(+) to CSA(−), both as is (B) and multiplied by a factor of 20 to match the excess amount of CSA(+) in the enantiomerically pure film (C).

to the vapors of *m*-cresol, the absorption spectrum shows the appearance of a free carrier tail of delocalized electrons. However, after secondary doping, there is no induced optical activity in the free carrier tail, accompanied by a disappearance of optical activity in the visible region. These results may be explained by *m*-cresol acting to "swell" the helix, facilitating a straightening out of the polymer chains, while mostly removing the chiral interaction with CSA.

Our results for *m*-cresol cast films, accompanied by results presented in the recent literature,[22] are inconsistent with this helix model applied to isolated chains. In these films, a large exciton-like splitting of the free carrier tail and a vibrational chirality corresponding to the emeraldine salt support the proposal that CDs comes almost exclusively from the tightly packed, highly crystalline regions. X-ray diffraction studies show the chains in the crystalline regions to be nearly planar with an interchain distance of 3.5 Å.[22,45] Furthermore, if the same interaction was taking place in films cast both from *m*-cresol and $CHCl_3$, the *m*-cresol would also be expected to fit the Q1D-VRH mechanism. Similar $\sigma_{dc}(T)$, $\sigma_{mw}(T)$, and anomalously long charge carrier lifetimes for *m*-cresol cast films doped with both chiral and achiral CSA point to the fact that the extent of charge transport is ultimately determined by transport through the achiral amorphous regions of the polymer film. We propose that a chiral interchain interaction, which is created by interaction between PAN, CSA, and *m*-cresol, is more likely, and that CSA(+) and CSA(−) segregate into groups to interact with PAN in solution, but the chiral interchain interaction in this case is made only after the solvent is evaporated. These results also explain observations by Wallace et al.[26] that unlike other solvents, PAN/CSA does not show optical activity when dissolved in *m*-cresol and that when *m*-cresol is added to $CHCl_3$ solutions, optical activity disappears. It is noted that the sensitivity of the PAN CD to the dopant, solvent, secondary dopant, and sample history may provide a basis for the use of PAN as a detector of chirality of chemical agents.

Acknowledgment. Supported in part by the Office of Naval Research, NSF:DMR-9508723, and NSF:CHE-9613861. Special thanks to Dr. Gordon Renkes for assistance with visible CD measurements.

CM011567X

(45) Pouget, J. P.; Hsu, C. H.; MacDiarmid, A. G.; Epstein, A. J. *Synth. Met.* **1995**, *69*, 119.